Spudich, J. A., & Watt, S. (1971) *J. Biol. Chem. 246*, 4866-4871.
Stossel, T. P., Chaponnier, C., Ezzell, R. M., Hartwig, J. H., Janmey, P. A., Kwiatkowski, D. J., Lind, S. E., Smith, D. B., Southwick, F. S., Yin, H. L., & Zaner, K. S. (1985) *Annu. Rev. Cell Biol. 1*, 353-402.
Sugino, H., & Hatano, S. (1982) *Cell Motil. 2*, 457-470.
Sutoh, K. (1982a) *Biochemistry 21*, 3654-3661.
Sutoh, K. (1982b) *Biochemistry 21*, 4800-4804.
Sutoh, K. (1983) *Biochemistry 22*, 1579-1585.
Sutoh, K. (1984) *Biochemistry 23*, 1942-1946.
Sutoh, K., & Mabuchi, I. (1984) *Biochemistry 23*, 6757-6761.
Sutoh, K., & Hatano, S. (1986) *Biochemistry 25*, 435-440.
Sutoh, K., Yamamoto, K., & Wakabayashi, T. (1984) *J. Mol. Biol. 178*, 323-339.
Towbin, H. M., Staehelin, T., & Gordon, J. (1979) *Proc. Natl. Acad. Sci. U.S.A. 76*, 4350-4354.
Toyoshima, C., & Wakabayashi, T. (1985a) *J. Biochem. (Tokyo) 97*, 219-243.
Toyoshima, C., & Wakabayashi, T. (1985b) *J. Biochem. (Tokyo) 97*, 244-263.
Vandekerckhove, J., & Weber, K. (1978a) *Proc. Natl. Acad. Sci. U.S.A. 75*, 1106-1110.
Vandekerckhove, J., & Weber, K. (1978b) *Eur. J. Biochem. 90*, 451-462.
Vandekerckhove, J., & Weber, K. (1978c) *Nature (London) 276*, 720-721.
Vandekerckhove, J., & Weber, K. (1984) *J. Mol. Biol. 179*, 391-413.
Vandekerckhove, J., Lal, A., & Korn, E. D. (1984) *J. Mol. Biol. 172*, 141-147.

α-Helix-to-Random-Coil Transitions of Two-Chain, Coiled Coils: A Theoretical Model for the "Pretransition" in Cysteine-190-Cross-Linked Tropomyosin†

Jeffrey Skolnick and Alfred Holtzer*
Department of Chemistry, Washington University, St. Louis, Missouri 63130
Received December 9, 1985; Revised Manuscript Received May 21, 1986

ABSTRACT: The thermal unfolding curve for $\alpha\alpha$ tropomyosin in which the two chains are cross-linked at cysteine-190 shows two striking features that distinguish it from that of its counterpart for non-cross-linked molecules: (1) a "pretransition" at 25–50 °C and (2) a shift in the principal transition to higher temperature, but with the same steepness. Previously, the pretransition was explained by postulating that the cross-link produces local strains, yielding a pinched "bubble" of chain-separated random coil about C-190, whereas the rest of the coiled coil remains intact. Results from both enzymatic digestion kinetics and equilibrium calorimetric studies have been interpreted as consistent with the existence of such a bubble. To test this idea further, a theoretical model is devised whereby various physical features can be imposed and the resulting helix content and other properties calculated from the statistical mechanical theory of the helix–coil transition. Short-range interactions employed are the geometric mean values of those in α-tropomyosin. The helix–helix interaction free energy is also like that in α-tropomyosin, including its nonuniformity; i.e., it is made larger in the amino half of the molecule. Local strain is introduced by setting the helix–helix interaction to zero in a region about the cross-link. The results show that, alone, neither local strain nor nonuniformity serves to mimic the experiments. In concert, however, they reproduce all the main experimental features, if the strain is extensive ($\sim$29 residues) and somewhat dissymmetric. Theoretical helix probability profiles, however, show that no bubble of unfolded chains forms about the cross-link. Instead, in the pretransition, residues unfold from the weakly interacting end (residue 284) in to, but not through, the cross-link at C-190. The theory also indicates that the augmented stability for the principal transition occurs largely as a result of loop entropy. The same strain and nonuniformity are then employed to explore the effects of other possible cross-link positions. The thermal curves are shown to depend markedly on cross-link location. The curves are discussed in terms of loop entropy, which has drastic, long-range effects. Under appropriate circumstances it can produce, in the coiled-coil model, a thermal transition that is essentially all or none.

Two-chain, coiled-coil proteins have a strikingly simple molecular architecture. The two constitutent polypeptide chains are each wound in an α-helix, the helices are set side by side in parallel and in register, and the pair is given a slight supertwist (Fraser & MacRae, 1973). The structural integrity of such molecules has been the subject of a great many investigations (Cohen & Szent-Györgyi, 1957; Noelken, 1962; Noelken & Holtzer, 1964; Woods, 1969; Halsey & Harrington, 1973; Chao & Holtzer, 1975; Lehrer, 1978; Williams & Swenson, 1981; Potekhin & Privalov, 1982; Holtzer et al., 1983; Graceffa & Lehrer, 1984; Skolnick & Holtzer, 1985; Stafford, 1985). This interest arises partly because the simplicity of the structure makes it an attractive model system for elucidation of structure-stabilizing interactions in proteins but also partly because local helix-to-random-coil transitions have often been postulated as essential biochemical events in

† Supported by Grant GM-20064 from the Division of General Medical Sciences, U.S. Public Health Service, and Grant PCM-82-12404 from the Biophysical Program of the National Science Foundation.

0006-2960/86/0425-6192$01.50/0

various functional processes in muscle and in other biological contexts as well (Lehrer & Betcher-Lange, 1979; Pepe, 1967; Harrington, 1979).

Among two-chain, coiled coils, tropomyosin has perhaps been most thoroughly studied in its unfolding transition. The best studied genetic variant of tropomyosin ($\alpha\alpha$) has 284 residues in each of two identical chains, each with a single cysteine, C-190 (Mak et al., 1979). Chain parallelism and registration in the native structure places the two cysteines in close enough juxtaposition so that oxidation yields an interchain disulfide cross-link (Johnson & Smillie, 1975; Lehrer, 1975; Stewart, 1975). The thermally induced helix–coil transition has been studied experimentally in such singly cross-linked molecules and differs in several significant ways from that observed in its non-cross-linked counterpart (Lehrer, 1978; Holtzer et al., 1983, 1986). These differences are the principal subject of this work.

One major difference lies in the dissociative nature of the transition in non-cross-linked tropomyosin, where the unfolded chains can separate, whereas in singly cross-linked molecules they cannot. This feature makes the transition concentration dependent in the non-cross-linked case (Holtzer et al., 1983; Isom et al., 1984; Yukioka et al., 1985; Stafford, 1985). However, since the cause of this difference in the transition is well understood to be a consequence of mass action, we will not allude to it further but simple employ, as a basis for comparison, the non-cross-linked protein at an intermediate concentration.

Non-cross-linked $\alpha\alpha$ tropomyosin shows a rather simple thermal unfolding profile (Figure 1, dashed curve) (Holtzer et al., 1983; Isom et al., 1984). Between 0 and ~30 °C there is a gradual decline in helix content from ~95% to 85%. Somewhat above 35 °C, there is a rather steep transition, which brings the helix content to 50% at ~46 °C and to only 12% at 55 °C. In contrast, the protein cross-linked at C-190 shows more complex behavior (Figure 1, solid curve) (Lehrer, 1978; Holtzer et al., 1983, 1986). Below 20 °C there is very little difference in shape, but between 25 and 50 °C the thermal curve for cross-linked material sags noticeably compared with that for its non-cross-linked counterpart. This sag has been referred to as a "pretransition" (Lehrer, 1978). It is followed by a much steeper, principal transition. The latter is about as steep as in the non-cross-linked case, considering an intermediate concentration of the latter, but displaced to higher temperature (50% helix at ~52 °C).

A proper physical picture of these transitions must explain these observed differences and describe how they are a necessary result of the introduction of the cross-link. At present, only a somewhat ad hoc explanation exists for the pretransition. It is postulated that in the undistorted native double helix the two sulfhydryls, which are each in the "a" interior position, cannot quite reach to form a disulfide bond and, moreover, that the structure has insufficient flexibility to allow such a bond. Formation of the disulfide therefore necessarily introduces a considerable steric strain in the helix, destabilizing it. Thus, it is considered that the pretransition consists of a local unfolding of the helix in the vicinity of C-190, where the cross-link is located (Lehrer, 1978). A picture of the cross-linked molecule at ~35 °C, say, would therefore show an intact, double-helical stretch at each end, separated (near C-190) by a pinched "bubble" of random coil centered at the cross-link (Graceffa & Lehrer, 1980; Betteridge & Lehrer, 1983).

Although this picture has intuitive appeal, it leaves unexplained why this local destabilization should *stabilize* the rest of the molecule. Attempts to test the picture directly by use of local spectroscopic probes have led to ambiguous results (Skolnick & Holtzer, 1985). Other relevant experimental approaches have involved studies of susceptibility to enzymatic digestion (Ueno, 1984) and differential scanning calorimetry (Williams & Swenson, 1981; Potekhin & Privalov, 1982), but both are strongly dependent on the interpretive methods employed to relate them to the relative equilibrium populations of conformational species.

The studies of enzymatic digestion kinetics have provided some support for the existence of a bubble but require not only difficult and uncertain experiments to analyze complex mixtures of fragments but a complex, mechanistic, chemical–kinetic interpretive scheme. Such schemes are never unique and depend critically on ones ability to guess the correct reaction path. In their equilibrium, calorimetric study of $\alpha\alpha$ tropomyosin, Potekhin and Privalov (1982) also accept the existence of a bubble. However, they assign the pretransition to two separate blocks, comprising residues 256–280 and 143–162, respectively. Since they also believe that residues 281–284 are never helical, the former block does not yield a bubble. The latter block does, but neither block is in the region of C-190. Potekhin and Privalov, in fact, conclude that the cross-link *strengthens* the structure in its own vicinity. However, the interpretation of these calorimetric studies has also been effected only by use of an arbitrary and model-dependent scheme designed to decompose the observations into a discrete number of quasi-independent steps. The result, as has been pointed out (Skolnick & Holtzer, 1985), is not only nonphysical but disagrees with light-scattering studies of molecular weight vs. temperature (Yukioka et al., 1985). Finally, objections to the bubble picture can be raised on theoretical grounds, as will be seen below.

In parallel with these experimental studies, a statistical mechanical theory of the thermal transitions has been developed (Skolnick & Holtzer, 1982a,b, 1985; Holtzer et al., 1983; Skolnick, 1983a,b, 1984, 1985a,b, 1986; Chen & Skolnick, 1986). This theory is very much in the spirit of the highly successful Zimm–Bragg (Zimm & Bragg, 1959) theory for the helix–coil transition in single-chain polypeptides. The latter had been extended to single chains of any known sequence and expresses the helix-stabilizing short-range interactions through helix initiation (σ) and propagation (s) parameters (Mattice, 1980). These have been experimentally measured for essentially all the amino acid residues occurring in proteins (Scheraga, 1978). Extension of the theory to two-chain molecules requires an additional parameter (w), which embodies the interhelix interactions that further stabilize the coiled coil. Initially given in somewhat crude form (Skolnick & Holtzer, 1982), the theory was soon augmented to include effects of out-of-register structures and of loop entropy (Skolnick, 1983a,b, 1984). Loop entropy assumes particular importance below. The term refers to the loss in entropy suffered by a randomly coiled chain when its ends are constrained to be close together and the number of conformations accessible to it thereby severely reduced. In its present form, the theory reproduces the principal features of the experimental findings in the case of non-cross-linked tropomyosin (Skolnick & Holtzer, 1985).

Recently, the formal theory has been extended to include singly and doubly cross-linked coiled coils (Skolnick, 1985a,b; Chen & Skolnick, 1986). In that endeavor it became clear that, even under the simplest circumstances, a cross-link can alter drastically the relative populations of the myriad molecular conformations possible in such a system. The resulting

thermal unfolding curves depend importantly on the position and number of such links. In good part, these effects come about as a result of loop entropy, which is an effect well established in polymer chemistry and of demonstrated importance in the study of conformational transitions in DNA and in globular proteins (Poland & Scheraga, 1970; Lin et al., 1985). Because a random coil suffers a severe loss in configurational entropy (and therefore reduction in stability) when it is closed into a loop, molecular conformations in which a cross-link is followed along the chains by randomly coiled segments and further on by a double-helical segment are inherently unstable. Yet, these are precisely like the bubble structure that has been postulated to explain the experimental pretransition in singly cross-linked tropomyosin.

In order to reconcile the ad hoc explanation of the experimental data with the statistical mechanical theory, we develop here a prototype theoretical model of the transition that allows easy computation yet at the same time mimics the essential features of the transition as found in tropomyosin. In this manner, one can quickly explore the effects of different assumptions concerning various physical features in the system in the hope of discovering which are necessary to reproduce the characteristic thermal curve found experimentally.

In this work, we focus particularly on physical features such as local instability caused by steric strain and the known nonuniformity in helix–helix interaction. It has been inferred (Skolnick & Holtzer, 1983) that stronger interhelix interactions at the amino-terminal half of tropomyosin account for its greater stability relative to the carboxy-terminal half (Woods, 1977; Pato et al., 1981). Such features, and others, can be independently controlled and varied at will in a theoretical model, whereas they are difficult or impossible to manipulate in any real experiment. Moreover, once the necessary features are defined so as to mimic the experiment, many details of the molecular configurational populations can be easily calculated that are at present impossible to measure. For example, given the physical assumptions needed to mimic the experimental curve of helix content vs. T, it is straightforward to calculate the corresponding helix probability profile, i.e., the fraction of helix as a function of position along the chain. This quantity is unavailable experimentally. As will be seen, this approach leads to an unequivocal specification of the underlying physical features required to produce a pretransition and to a reinterpretation of its conformational properties.

Methods and Models

Consider a hypothetical two-chain, coiled coil containing N_B α-helical turns or blocks, where each block contains m residues and where each chain is numbered from the the N to the C terminus. As usual, we assume that the short-range interactions are adequately represented by the Zimm–Bragg helix initiation (σ) and propagation (s) parameters. The value assigned to each parameter is the same for each residue in the chain and equal to the geometric mean value ("effective value") found in tropomyosin (Skolnick & Holtzer, 1982b), namely, $\sigma_{eff} = 5.0 \times 10^{-4}$ and

$$\ln s_{eff}(T) = B_0 + B_1 T^{-1} + B_2 T^{-2} \quad (1a)$$

where T is in kelvin and

$$B_0 = -3.914\,506\,27 \quad (1b)$$

$$B_1 = 2\,207.203\,86 \quad (1c)$$

and

$$B_2 = -314\,920.425 \quad (1d)$$

In this scheme, then, regional variations in short-range interactions are averaged.

Long-range interactions are accounted for by the helix–helix interaction parameter $w(T)$ introduced previously (Skolnick & Holtzer, 1982a, 1985; Holtzer et al., 1983). Physically, $-kT \ln w$ is the free energy of a pair of positionally fixed and interacting, side by side α-helical turns minus that of the positionally fixed, noninteracting pair of α-helical turns. In some of the calculations discussed below, regional variations in $w(T)$ within a molecule are included. Such variations are known to be present in α-tropomyosin wherein the interaction is stronger in that half of the molecule containing the amino terminals (Pato et al., 1981; Skolnick & Holtzer, 1983). In those cases, we designate a point between block NN and block NN + 1 as the boundary between the more and less stable portions of the coiled coil. The helix–helix interaction parameter between block i in chain one and block j in chain two is written as

$$w_{ij} = w_N \quad (2)$$

if both $i \leq NN$ and $j \leq NN$, i.e., if both interacting blocks are in the strongly interacting region of their own chain; whereas, we write

$$w_{ij} = w_C \quad (3)$$

if $i > NN$ and $j > NN$, i.e., if both are in the weakly interacting region. In the non-cross-linked case, where out-of-register conformations of the chains are important, consideration must be given to interactions between strongly interacting and weakly interacting blocks. For such interactions, we employ the geometric mean of the like-pair interaction (Holtzer et al., 1984):

$$w_{ij} = (w_N w_C)^{1/2} \quad (4)$$

To obtain actual numerical values of the interaction parameters, we employ relations previously developed for tropomyosin (Holtzer et al., 1983; Skolnick & Holtzer, 1985). Specifically, for w_C we write

$$RT \ln w_C = BT \ln T + A_0 + A_1 T \quad (5a)$$

with R in cal·K^{-1}·(mol of block pairs)$^{-1}$, and

$$B = 52.627\,425\,9 \quad (5b)$$

$$A_0 = 15\,743.499\,8 \quad (5c)$$

and

$$A_1 = -351.163\,555 \quad (5d)$$

To obtain w_N, we write

$$RT \ln w_N = RT \ln w_C + 250.00 \quad (5e)$$

That is, we provide a free-energy difference of 250 cal·(mol of block pairs)$^{-1}$ between the strongly and weakly interacting regions of the coiled coil. This is within the plausible range of regiospecific variations in w in tropomyosin (Skolnick & Holtzer, 1983). In each case, the temperature dependence also follows that found in tropomyosin (Skolnick & Holtzer, 1985).

Since it is instructive to compare such nonuniformly interacting coiled coils with uniform counterparts, it is also necessary to choose interaction parameters for uniform coiled coils. To this end, we use an algorithm for $RT \ln w(T)$ that is identical with that found by the fit, on the assumption of uniformity, to the experimental thermal denaturation profiles of α-tropomyosin at neutral pH (Skolnick & Holtzer, 1985). This algorithm follows eq 5a, 5b, and 5d but employs $A_0 = 15\,793.499\,8$ instead of eq 5c. We thus employ a uniform shift of 50 cal between uniform and nonuniform models. This shift in interhelical free energy is necessary to produce a thermal

transition in the nonuniform model system that occurs in approximately the same temperature range as that in α-tropomyosin. This shift is only $\sim$10% of the total interaction free energy.

The procedure for calculating the overall helix content for non-cross-linked chains is summarized in eq 1–9 of section II of Skolnick and Holtzer (1985). In the calculations presented below, we have summed over all out-of-register states, rather than excluding the salt–hydrophobe contacts as in eq 9 of the reference. This has no effect whatsoever on the conclusions that follow. To calculate the fraction of residues that are helical, ϕ_h, we need to specify C_0, the total molar concentration of protein in formula weights of chains per liter of solution, and u, the effective volume in configurational space accessible to the center of mass of one interacting α-helical turn in the coiled coil species when the α-helical turn in the other chain is held fixed. We have arbitarily taken u = 359 Å; a discussion of the plausibility of this value is found in Skolnick and Holtzer (1985).

Turning to the case of singly cross-linked chains, we assume that the m_lth residue of block pair N_x contains a cross-link, and below we examine two possible effects of the cross-link on the intrinsic stability of the coiled-coil structure. First, we assume that the cross-link is completely benign and leaves w, σ, and s in the vicinity of the cross-link unchanged from the non-cross-linked case. Second, we assume that the local geometric constraints imposed upon the coiled-coil structure by the formation of the cross-link are so severe that blocks $N_x - \Delta_1$ through $N_x + \Delta_2$ experience no enhanced helical stability whatsoever over that of the separated chains. That is

$$\text{if } N_x - \Delta_1 \leq i \leq N_x + \Delta_2, \quad \text{then } w_{ii} = 1 \qquad (6)$$

otherwise w_{ii} is the same as that in the non-cross-linked case. Thus, we allow the strain due to cross-link formation to extend for $\Delta_1 + \Delta_2 + 1$ blocks. In this way the effects of the range of the disruption can be investigated. Moreover, by allowing for the possibility that $\Delta_1 \neq \Delta_2$, the effect of a dissymmetry in strain can also be studied. In the Appendix, we consider the possibility that the strain actually leads to helix–helix repulsion, i.e., that $w_{ii} < 1$.

Observe that in writing eq 6 for cross-linked molecules we only include interacting conformations of the two chains that are in register. Recent theoretical work indicates that mismatched (i.e., out-of-register) states in singly cross-linked molecules can be entirely neglected; because they require the formation of a constrained interior random-coil loop at the cross-link, such states pay a heavy entropic price and are unimportant (Chen & Skolnick, 1986). In fact, it has been shown that either the cross-linked pair of blocks are helical and interacting or the molecule has no interacting pairs of helices at all (Skolnick, 1985b).

In order to calculate the overall helix content in a singly cross-linked molecule, we have to specify, in addition to the quantities indicated above, a configurational factor, r_ϕ, that bears a certain analogy to the parameter u employed for the non-cross-linked case. Physically, r_ϕ is the ratio of the effective volume available in configurational space to the cross-linked pair of blocks in the interacting conformation to that in the noninteracting conformation, and it includes the contribution of the configurational entropy of the cross-link itself. The overall helix content of a singly cross-linked coiled coil was calculated via eq II-8a-b of Skolnick (1985b). The helix probability profile was calculated via eq II-13 of the same work.

In the calculations presented below, we have set N_B = 81, m = 4, m_l = 3, r_ϕ = 0.1, and NN = 38. These parameters

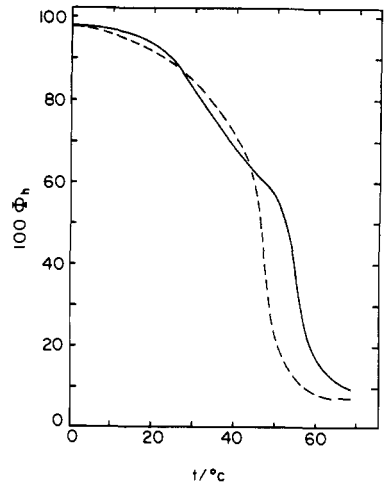

FIGURE 1: Experimental thermal unfolding curves (percent helix from circular dichroism vs. temperature) for $\alpha\alpha$ tropomyosin in 0.5 M NaCl–50 mM NaP_i, pH 7.4: (dashed curve) spline curve through extant data for non-cross-linked species at 0.104 mg/ml; (full curve) spline curve through extant data for C-190-cross-linked species.

are chosen so that the number of α-helical turns is the same as in tropomyosin. Similarly NN = 38 splits the molecule into two regions of different stability such that the fraction of residues in each region is the same as in the T-1 and T-2 fragments of tropomyosin (Pato et al., 1981; Skolnick & Holtzer, 1983).

Although these block designations are fundamental to the theoretical calculation, it is not customary to employ them in biochemical studies. Most readers are more accustomed to locating a point within the tropomyosin chain by its residue number in the conventional sense, wherein the amino terminus is number 1 and the carboxyl terminus number 284. For this reason, the discussion below will avoid block designations wherever possible. Thus, the strongly interacting region will be understood to include residues 1–133 and the weakly interacting region residues 134–284; cross-linking will be referred to as at C-190, etc. We believe that examination of this tropomyosin analogue, in which short-range interactions are replaced by their average values, can be instructive, because the ease of computation allows relevant features to be varied and their effects rapidly assessed.

Results and Discussion

Empirical Basis of the Investigation. As already noted, the experimental facts underlying this study are displayed in Figure 1 as spline curves through the extant data for non-cross-linked (dashed) and C-190-cross-linked (solid) $\alpha\alpha$ tropomyosin. The curve for non-cross-linked protein is for a tropomyosin concentration of $\sim$0.1 mg·cm^{-3}, which is at an intermediate point within the experimentally accessible range ($\sim$0.005–5.0 mg·cm^{-3}). In our discussion, such an intermediate concentration will always be meant whenever curves for "non-cross-linked" protein are under consideration. This weight concentration of tropomyosin corresponds to a formal concentration of $\sim 3.2 \times 10^{-6}$ mol of polypeptide chains per liter of solution.

The thermal curve for non-cross-linked protein is relatively featureless. With increasing T, the helix content drifts downward slowly ($\sim$0–40 °C) and then displays a steeper drop (40–55 °C) in which most of the helix content is lost. In contrast, the curve for C-190-cross-linked material shows a peculiar and characteristic shape. It shows an initial shallow decline ($\sim$0–25 °C), a subsequent sag, called the "pretransition", which indicates a destabilization ($\sim$25–50

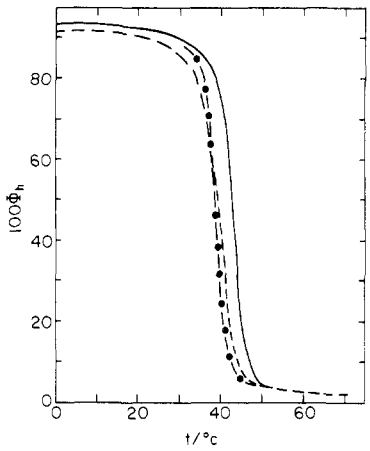

FIGURE 2: Theoretical thermal unfolding curves (percent helix vs. temperature) showing effect of local strain near the cross-link in a molecule with uniform interhelix interaction: (dashed curve) non-cross-linked species (at 0.104 mg/mL); (full curve) C-190-cross-linked species with 7,21 strain; (dot–dashed curve) C-190-cross-linked species with 21,21 strain.

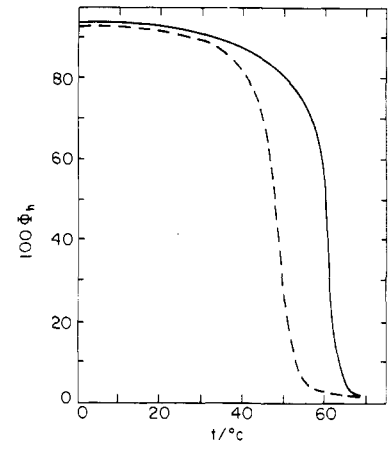

FIGURE 3: Theoretical thermal unfolding curves (percent helix vs. temperature) showing effect of nonuniform interhelix interaction (residues 1–133, strong; residues 134–284, weak) in a molecule with no local strain near the C-190 cross-link: (dashed curve) non-cross-linked species (at 0.104 mg/mL); (full curve) C-190-cross-linked species.

°C), and finally a steep loss of helix (50–65 °C). The temperature of 50% helix is ~52 °C, appreciably higher than the 46 °C seen for non-cross-linked protein.

Essential features requiring explanation in the cross-linked case thus are (1) the sag at intermediate temperature, i.e., the pretransition, and (2) the increase in characteristic temperature but similarity in slope of the principal transition compared with non-cross-linked protein. The small difference in the curves below room temperature may or may not be a third significant feature. It is hard to say at present because the differences are, percentagewise, rather small. Moreover, the CD measurements below room temperature are somewhat less certain. Thus, the observed differences in this region are comparable to experimental errors. It is noteworthy that these general, comparative features of the curves are independent of the particular ways of converting the observed CD into helix content and have been confirmed by measurements in different laboratories.

Uniform Helices, Unstrained and Strained. Since it is our purpose to investigate the effects of nonuniformity in helix–helix interaction along the chain and of steric strain local to the cross-link, four possibilities require examination. The coiled coils may be uniform and unstrained, uniform and strained, nonuniform and unstrained, or nonuniform and strained. In this section we consider both types of uniform coiled coils.

The simplest case is of a uniform chain with no strain attendant upon creation of the cross-link, which becomes a simple tether. Since the existence of the tether not only prevents dissociation but alters the population of states in other ways—for example, by effectively eliminating out-of-register states—one cannot eliminate a priori the possibility that the peculiar features of the curve for cross-linked molecules may be explained on this basis alone. However, calculations have already been reported for this case, and they show that no such peculiar features appear (Skolnick, 1985b). The uniform, unstrained, cross-linked molecule shows a thermal curve that is relatively featureless and always *above* the curve for its non-cross-linked counterpart. In this case, the effect of a simple tether joining uniform chains is essentially equivalent to raising the chain concentration to a very high value, as perhaps might have been anticipated (Creighton, 1983).

The effect of a destabilizing strain at the C-190 cross-link in a molecule with uniform helix–helix interaction is shown in Figure 2. Here again, the (dashed) thermal curve for the corresponding non-cross-linked molecule is compared with those of the molecules containing, this time, a strained cross-link. Two examples of the latter are shown. In one case (dot–dashed curve), a rather extensive, symmetric strain—ranging 21 residues on each side of the cross-linked residue, a so-called 21,21 strain—is introduced. In the second case (full curve), a lesser, dissymmetric strain is introduced, extending 7 residues on the amino-terminus side and 21 on the carboxyl-terminus side, i.e., a 7,21 strain. Neither yields a thermal curve with the complexity seen experimentally. No sagging pretransition region appears. Although the curve for the large symmetric strain crosses that for non-cross-linked protein, it does so from above. Indeed, this is a necessary consequence of the existence of less helical out-of-register conformations in the non-cross-linked molecules. As noted above, such conformations are absent in the cross-linked molecule. These conformations decrease the helix content when it is high and increase it when it is low (Skolnick, 1985b). In addition to the examples given, we have investigated a variety of other types of local destabilizations, with the same result. Given uniform helix–helix interaction elsewhere, no destabilization of reasonable range initiating at the C-190 cross-link gives thermal curves that mimic the experimental ones. We are therefore forced to consider molecules with nonuniform interhelix interactions.

Nonuniform Helices, Unstrained and Strained. We next inquire whether nonuniformity in interhelix interactions alone can explain the experiments. In Figure 3, the theoretical curve for the nonuniform, non-cross-linked molecule (dashed curve) is compared with its counterpart (full curve) containing an unstrained cross-link at C-190. Again, the results do not mimic the experimental findings. The simple, unstrained tether, in the nonuniformly as in the uniformly interacting case, acts to raise the helix content at every T; i.e., it merely produces an effect equivalent to a large increase in concentration.

It is therefore necessary to consider the possibility that both nonunformity and local strain are essential features of the thermal curve in the cross-linked system. The result of a theoretical calculation that includes both features is given in Figure 4, whence it is seen that all the essential features of the experimental curves are effectively mimicked if the strain extends 7 residues to the amino-terminus side of C-190 and 21 residues to the carboxyl side, i.e, a 7,21 strain. It is

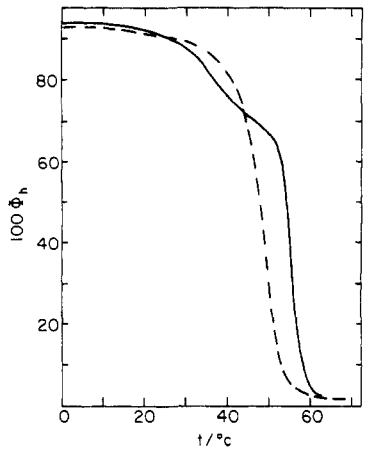

FIGURE 4: Theoretical thermal unfolding curves (percent helix vs. temperature) showing nonuniform interhelix interaction (residues 1–133, strong; residues 134–294, weak) and local strain near the C-190 cross-link appropriate to mimic the experiments of Figure 1: (dashed curve) non-cross-linked species (at 0.104 mg/mL); (full curve) C-190-cross-linked species with 7,21 strain.

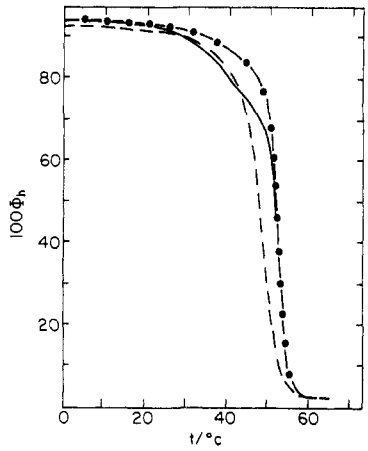

FIGURE 5: Theoretical thermal unfolding curves (percent helix vs. temperature) showing nonuniform interhelix interaction (residues 1–133, strong; residues 134–284, weak) and local strain near the C-190 cross-link inappropriate to mimic the experiment of Figure 1: (dashed curve) non-cross-linked species (at 0.104 mg/mL); (full curve) (C-190-cross-linked species with 18,18 strain; (dot–dashed curve) C-190-cross-linked species with 21,7 strain.

noteworthy that the calculated curves shown in Figure 4 show not only the essential features but also the crossover at low temperature, encouraging the belief that this feature is, in fact, real. However, an experimental test would require rather exacting measurements.

Some idea of the effects of alterations in the precise nature of the local strain may be obtained from Figure 5, wherein calculations are shown for a large but symmetric (18,18) strain (full curve) and for a strain (21,7) of the same extent as, but opposite in symmetry to, that in Figure 4 (dot–dashed curve). Although the symmetric strain is larger (37 residues) than that given in Figure 4 (29 residues), it does not give a pretransition of the right magnitude, shows too small a $\Delta T_{1/2}$, and gives a slope in the region of the principal transition that is too large to mimic the experiments. The curve with 21,7 strain—i.e., reversed compared with Figure 4—is even less satisfactory; it shows no pretransition at all.

The results of Figure 5 thus indicate that the strain introduced by the cross-link in the nonuniform molecule may be biased as it proceeds outward from C-190. The theory suggests that it proceeds further in the direction toward the nearest open chain end. We believe this is physically reasonable in that a

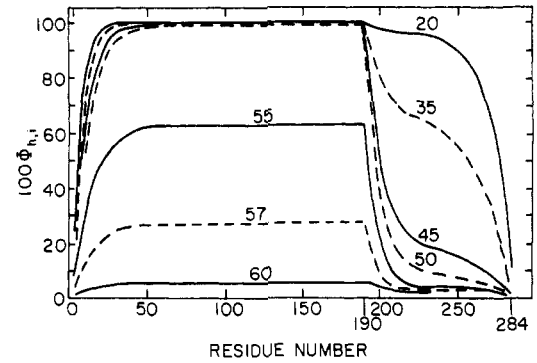

FIGURE 6: Theoretical helix probability profiles for C-190-cross-linked species with nonuniform interhelix interaction (residues 1–133, strong; residues 134–284, weak) and 7,21 strain at the cross-link. Curves show percent helix as a function of residue position. Temperatures as marked in °C. Curves are alternately dashed or full to promote contrast.

stress is likely to result in a greater strain toward the structurally weaker side of the stressed point. This idea will be discussed further below.

Molecular Conformational Interpretation of the Transition. We have established the physical conditions required in order that the model mimic the data. These include nonuniform interhelix interaction along the chains and a substantial, somewhat dissymmetric, destabilization local to the cross-link. Having determined these necessary input conditions, we can now employ the theory to derive the molecular conformational characteristics of the transition. To this end, we employ the helix probability profile, i.e., the mean helix content as a function of residue number along the chain. Given the input parameters, this quantity is calculated from the theory in a straightforward manner (Skolnick, 1985b).

Figure 6 displays these profiles at a series of temperatures for the cross-linked molecule whose thermal curve is given in Figure 4, i.e., the one that mimics the experimental data. The reader is reminded that such a profile for a non-cross-linked, homopolymeric molecule is essentially constant over a long stretch near the middle of the molecule, declining steeply at either end. This unraveling at the ends is a well-understood statistical effect. With increasing T and therefore decreasing helix content, the constant central region is simply lowered.

The results for the relevant cross-linked molecule (Figure 6) are quite different and provide insight into the molecular nature of the peculiar thermal transition it displays (Figure 4). The profiles in the termperature region of the pretransition (consider especially 35, 45, and 50 °C in Figure 6) plainly show that the molecule in this region denatures from its weakest interacting (carboxyl) end in to, *but not through*, the cross-link. Thus, no bubble of random coil forms about the stress-weakened region. Such conformations are suppressed by their unfavorable (loop) entropy. A bubble would appear on the curves as a depressed region around the cross-link. There is no such region.

As T is raised further, we pass into the region of the principal transition (55, 57, and 60 °C on Figure 6). In this entire region, the molecule from the C-190 cross-link to the carboxyl chain ends essentially comprises two chain-separated random coils. As we traverse the principal transition, the helix content from the amino end to the cross-link suffers a steady decline, the observed value being an average over many conformations.

In essence, then, the theory presents the following picture of the transition in the C-190-cross-linked system. Given the nonuniformity and strain necessary to mimic the observed thermal curve, the theory insists that the cross-link essentially

divides the transition into two stages: (1) the pretransition in which the coiled coil unfolds from the weakly interacting end to the cross-link and (2) the principal transition in which the molecule unfolds more or less uniformly from the strongly interacting end in to the cross-link, with molecules that have appreciable helix content and contain interacting segments in equilibrium with noninteracting molecules that are much more unfolded and contain no interacting segments.

It is particularly noteworthy, and goes to the heart of the matter, that no special features appear in the profiles of Figure 6 at residues 133–134, where the boundary between strongly and weakly interacting regions exists. One might have expected unfolding on the weakly interacting side, from the C-terminus to residue 133, followed and somewhat overlapped by unfolding from the N-terminus. That this does not occur is, again, due to loop entropy. At 50 °C, say, the region of residues 1–133 is highly helical because of its strong interactions. Because of the cross-link at residue 190, the region 133–190 is thus perforce helical as well, for otherwise an enormous randomly coiled loop would be created between the strongly interacting pair of residues at 133 and the cross-link at 190. That is why the mean helix content at residue 150, say, in the weakly interacting region is essentially no different from that at, say, 115 in the strongly interacting region.

This physically long-range effect of loop entropy is perhaps also the reason why we observe some dissymmetry in the strain. If the molecule is stressed by cross-link formation at C-190, it cannot gain relief by a strain produced from there toward the amino end, for, as just seen, loop entropy compels that region to be a coiled coil so long as the coiled coil persists at the very stable amino end. Thus, relief *must* be gotten at the expense of helix content from the cross-link to the nearest *open* end, in this case the carboxyl end.

Nonuniform, Strained Helices Cross-Linked at "C-95". Accepting the nonuniformity of the tropomyosin coiled coil and the kind of strain the cross-link introduces, we explore further the effects of such cross-links on thermal transitions by examining the effects of a cross-link placed in the strongly interacting region, instead of the weakly interacting one. Since it has been shown theoretically that even in the case of a uniform, homopolymeric coiled coil with an unstrained cross-link the residue position of the cross-link can have pronounced statistical effects on the transition (Skolnick, 1985b), we place the cross-link at residue 95. We will refer to this as a "C-95" cross-link, since tropomyosin has no actual cysteine at that point. This puts it at the same distance from the amino end as residue 190 is from the carboxyl but quite amidst the strongly interacting region, just as 190 is amidst the weakly interacting region. Likewise, the strain is of the 21,7 type, i.e., identical in magnitude and dissymmetry as for the 190-crosslinked molecule; however, here we give the dissymmetry the opposite algebraic sign, in this case directing the strain more toward the amino terminus, the nearest *open* end, in accord with the discussion above.

The resulting thermal curve is shown dotted on Figure 7A, where it may be compared with those already discussed for non-cross-linked (dashed curve) and C-190-cross-linked (full curve) molecules. The "C-95"-cross-linked molecule shows no pretransition whatever, but its temperature of half-unfolding (~48 °C) is appreciably lower than that for the C-190-cross-linked species (~54 °C).

The underlying molecular conformational reasons for this are made plain by the corresponding helix probability profiles (Figure 8). Here, the strong interaction at the amino end forbids a short-end-to-cross-link pretransition like the one seen

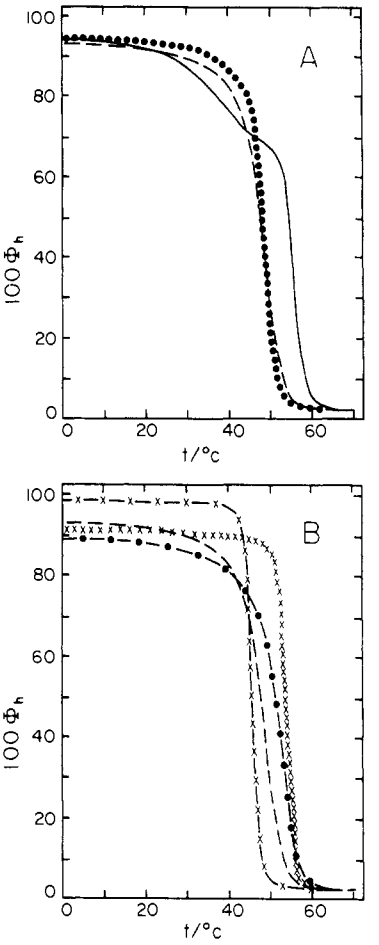

FIGURE 7: Theoretical thermal unfolding curves (percent helix vs. temperature) for various species. All have nonuniform interhelix interaction (residues 1–133, strong; residues 134–284, weak). (Dashed curve in each case) Non-cross-linked species (at 0.104 mg/mL). (A) (Full curve) C-190-cross-linked species with 7,21 strain; (dotted curve) "C-95"-cross-linked species with 21,7 strain. (B) (Dot–dashed curve) C-36-cross-linked species with 21,7 strain; (×ed curve) "C-249"-cross-linked species with 7,21 strain; (×–dashed curve) "C-284"-cross-linked species with 25,0 strain.

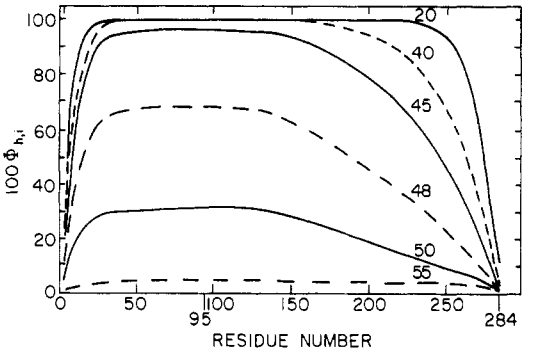

FIGURE 8: Theoretical helix probability profiles for "C-95"-cross-linked species with nonuniform interhelix interaction (residues 1–133, strong; residues 134–284, weak) and 21,7 strain at the cross-link. Curves show percent helix as a function of residue position. Temperatures as marked in °C. Curves are alternately dashed or full to promote contrast.

at the carboxyl end in the C-190-cross-linked species. Thus, at intermediate temperature, the helix content for the "C-95"-cross-linked species is greater. However, Figure 8 makes plain that the weakly interacting region (residues 133–190) is no longer loop-entropy stabilized, because now there is no cross-link at C-190. Hence, in the "C-95"-cross-linked species, as temperature rises, the weakly interacting residues can freely

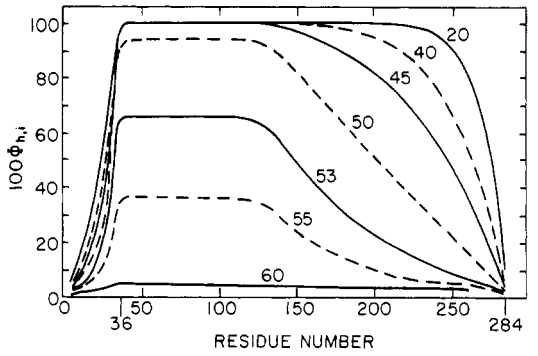

FIGURE 9: Theoretical helix probability profiles for C-36-cross-linked species with nonuniform interhelix interaction (residues 1–133, strong; residues 134–284, weak) and 21,7 strain at the cross-link. Curves show percent helix as a function of residue position. Temperatures as marked in °C. Curves are alternately dashed or full to promote contrast.

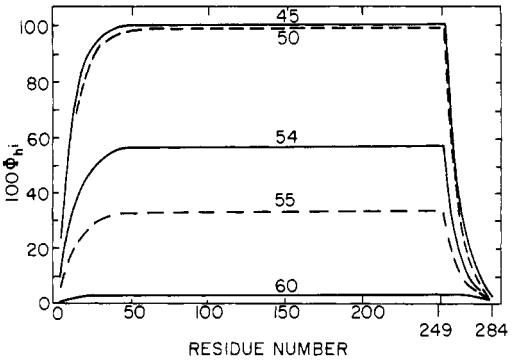

FIGURE 10: Theoretical helix probability profiles for "C-249"-cross-linked species with nonuniform interhelix interaction (residues 1–133, strong; residues 134–284, weak) and 7,21 strain at the cross-link. Curves show percent helix as a function of residue position. Temperatures as marked in °C. Curves are alternately dashed or full to promote contrast.

unfold from the carboxyl end all the way to residue 133. Strong loss of helix in the region 133–284, in concert with gradual loss in the strongly interacting region, thus conspires to reduce the helix content below that found in the C-190-cross-linked case. Thus, the "C-95"-cross-linked molecule, not possessing a vulnerable, weakly interacting, 94-residue peptide between the cross-link and the nearest end, shows no pretransition but simply melts in from both ends toward the cross-link, albeit more drastically from the weakly interacting end.

Nonuniform, Strained Helices Cross-Linked at C-36. Since there is a genetic variant of the tropomyosin chain that has a cysteine at position 36, it is also of interest to inquire as to the expected effect of a single cross-link at that site. Using the same nonuniformity and the anticipated 21,7 strain, we find the thermal transition shown as the dot–dashed curve of Figure 7B. Qualitatively, the behavior is similar to that in the "C-95"-cross-linked material. Although the details differ, there is no pretransition, and the principal transition is at lower temperature than for the C-190-cross-linked species.

The molecular situation in the C-36-cross-linked species is clarified by reference to Figure 9, wherein are shown some helix probability profiles. Those at lower temperature (20 and 40 °C) reveal that the cause of the relatively low helix content for this species in this region lies in the extreme vulnerability to unfolding of the 36-residue peptide between the amino terminal and the cross-link. This is due to its small size relative to the range of the strain and to the conformational isolation the cross-link forces upon it. On the other hand, the *augmented* stability of the C-36- over the "C-95"-cross-linked species at higher temperature is again clearly a result of a combination of loop entropy, which constrains interacting helical regions to include the cross-link, and of the greater extent, in the C-36-cross-linked species, of the range from the cross-link to the beginning of the weakly interacting region. In the C-36-cross-linked species, strongly interacting residues from 36–133 remain highly helical up to elevated temperature. In the "C-95"-cross-linked species, this region is drastically reduced, ranging from 95 to 133. From the overall qualitative viewpoint, however, the "C-95"- and the C-36-cross-linked transitions are similar. Both species unfold in from the ends to the cross-link. This prediction concerning the thermal transition in the C-36-cross-linked species could be tested with $\beta\beta$ tropomyosin, if a way can be found to block C-190 selectively so that the molecule can be cross-linked at C-36 only.

Nonuniform, Strained Helices Cross-Linked at "C-249" and at "C-284". It is instructive to compare the result for the C-36-cross-linked species with its symmetrical analogue, the coiled coil having a cross-link at (fictitious cysteine) residue 249, the same distance from the opposite (carboxyl) end. This residue is thus very near the *weakly* interacting end. In view of our prior discussion, we again expect an incomplete helix even at low temperature, because the 7,21 strain extends virtually from the cross-link to the carboxy end, so that peptide segment always has low helix content. Now, however, the weakly interacting peptide in the region between strongly interacting segments and the cross-link (134–249) is enlarged. As a result, loop entropy has a remarkable stabilizing effect on the unfolding curve, as shown on Figure 7B (×ed curve). The result of these topological constraints is a highly stable molecule, but one which undergoes a highly cooperative transition once a high-enough temperature has been reached. The profiles shown for this case in Figure 10 demonstrate this interpretation further.

These long-range effects of toplogical constraints, acting through loop entropy, can be seen even more strikingly if this loop-entropy-stabilized region is further extended by moving the cross-link all the way out to the chain end at residue 284. The result of a 25,0-strained cross-link at that point is also seen on Figure 7B (×–dashed curve). The molecule is virtually completely helical at low temperature, but displays, at rather high temperature, a remarkable, highly cooperative transition that is highly reminiscent of those encountered in globular proteins, where such constraints are the rule. This points up how loop entropy, acting in concert with interchain, region-specific interactions, can produce an essentially two-state transition in which almost fully helical species exist in equilibrium with essentially completely unfolded forms.

Conclusions

Briefly stated, the statistical mechanical theory of the thermal transition in cross-linked coiled coils can explain the peculiarities of the experimental curve for C-190-cross-linked tropomyosin, including the appearance of a pretransition at intermediate temperature and the deferral of the principal transition to much higher temperature. These features emerge if and only if the following are inserted into the physics.

(1) The helix–helix interaction must be nonuniform along the chain, in the manner, and of an approximate magnitude, known to hold in tropomyosin. That is, the amino-terminal segment must have a helix–helix interaction larger, per pair of α-helical turns, by a few hundred calories than that of the carboxy terminal.

(2) The cross-link must be assumed to introduce a destabilizing strain about C-190. This strain must extend rather

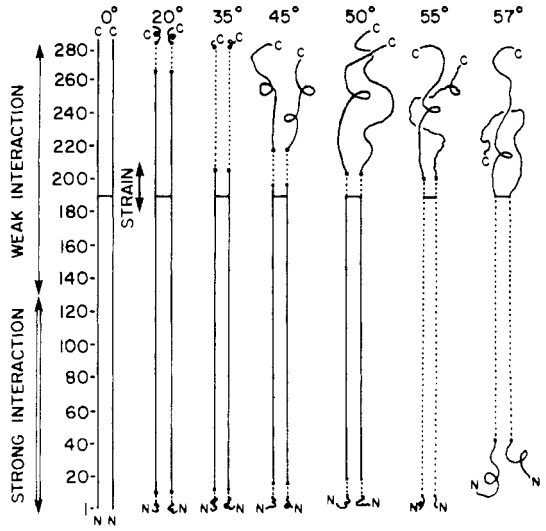

FIGURE 11: Pictorial representation of molecular conformation of C-190-cross-linked species from the theoretical model that mimics experiments, i.e., using results of Figure 6. Segments >75% helical are shown as straight parallel lines, segments between 25% and 75% helical as dotted lines, and segments <25% helical as chain-separated random coils. Temperature as marked. Position of cross-link and range of strong interactions, weak interactions, and strain are also shown.

far and is probably more extensively manifest in the carboxyl direction from C-190. Our theoretical model fits best with a strain extending 7 residues in the N-terminal and 21 in the C-terminal directions, but such estimates must be taken as very rough because of the various arbitrary features of the model.

It is evident that this second feature is precisely the one suggested earlier on ad hoc physical grounds by Lehrer (1978), who discovered the pretransition. However, the ad hoc molecular interpretation of the pretransition—as resulting in a C-190-centered bubble of random coil flanked on either side by intact coiled-coil segments—does not survive scrutiny. According to the present theory, loop entropy makes such conformations immaterial. Helix probability profiles show that in the pretransition, instead of forming a bubble, the molecule unfolds essentially from the carboxyl end in to the cross-link. It might be conjectured that bubble-containing conformations could be stabilized if a strain is employed in which the local helix–helix interaction is made sufficiently *repulsive* (i.e., $w < 1$). The incorrectness of this idea is amply demonstrated in the Appendix. We believe that a good grasp of the conformational implications of the theory may be gained by perusal of the heuristic calculation in the Appendix.

The theory also explains the deferral of the principal transition to higher temperature. This increased stability of the remaining molecule comes about largely because the strong double helix at residues 1–133, acting in concert with the cross-link at 190 and loop entropy, keeps relatively weakly interacting residues 134–190 helical to higher temperatures than in the corresponding non-cross-linked species.

Some sense of the conformational stages predicted for the C-190-cross-linked species can be obtained from Figure 11, wherein segments greater than 75% helical are represented by a pair of straight parallel lines, segments between 25% and 75% helical by dotted parallel lines, and segments less than 25% helical by chain-separated, thread-like coils. However, the reader is warned that these are rough guides only and must not be interpreted as displaying a single species that is dominant at the given temperature. It is a particular requirement of the statistical mechanics that these drawings represent very rough averages over a broad spectrum of allowed states.

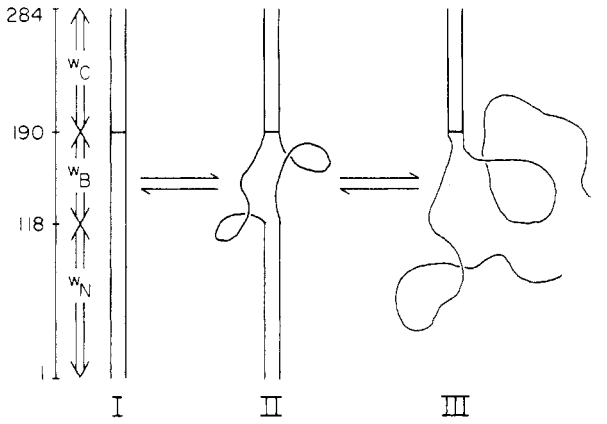

FIGURE A1: Pictorial representation of prototypical conformational equilibria for C-190-cross-linked tropomyosin at 35 °C. Residue number is indicated by scale at left. Helical blocks comprising residues 1–118 are characterized by the attractive interhelix interaction parameter w_N(35 °C), those with residues 119–189 (the bubble region) by the repulsive parameter w_B(35 °C), and those with residues 190–284 by the attractive parameter w_C(35 °C). Straight, parallel lines designate interacting double α-helical (coiled-coil) chain segments. Meandering lines designate randomly coiled chain segments.

We believe the present theory can be useful in interpreting thermal transition data in coiled coils. As seen above, once the model yields a thermal curve that mimics the experimental one, the calculated helix probability profile then reveals the appropriate interpretation in molecular conformational terms. Unfortunately, it is very difficult to go the reverse way; i.e., start with a few qualitative ideas (loop entropy, localized strain, etc.) and predict the general features by qualitative arguments only. It is simply too uncertain to guess what relative weights the various competing effects will have, without actually evaluating the theoretical expressions numerically. This makes interpretation difficult, but we believe it is inherent to the physical system itself, not a deficiency of the present approach. It remains to be seen whether the predictions generated by this approach will be confirmed by experiment and whether the theory can be extended successfully to coiled coils with more than one cross-link. Some data for doubly cross-linked coiled coils are already extant (Holtzer et al., 1986).

ACKNOWLEDGMENTS

We thank Drs. Sherwin Lehrer and David Williams, Jr., for a provocative discussion of this work. Indeed, the incentive to perform the analysis and calculations in the Appendix was provided by their tenacious questioning concerning the content of the theory.

APPENDIX

Heuristic Demonstration of Bubble Instability. It is tempting to attempt to legislate bubbles by further increasing the strain in the region of the cross-link, thereby creating a locally *repulsive* interaction between helices. A referee and several others have made this suggestion, which has intuitive appeal. Although, as shown below, it is a self-defeating strategy, considerable insight may be gained in the process.

The issue can be clarified by selecting a few, prototypical structures and examining equilibria among them. This process allows examination of the question while avoiding the complex and cumbersome array of summations that accompany any discussion in which the entire spectrum of molecular conformational states is spanned. The prototypical structures shown in Figure A1 can serve as a basis for such a skeleton discussion.

Note that conformer I is an intact, double α-helical, coiled coil, while II has a bubble of random coil on the N-terminus

side of the cross-link. It is often postulated that, at 35 °C (i.e., well into the pretransition), conformers like I and II are the only important ones, the dominance of those like II being the essential cause of the loss of helix in the pretransition (Graceffa & Lehrer, 1980; Betteridge & Lehrer, 1983; Lehrer, 1986). Since the helix content at 35° C is ~75%, it may be supposed that the randomly coiled bubble in II comprises ~284/4 = 71 residues on each chain. Structure III will also be considered for reasons that will soon become apparent. We next describe more explicitly the characteristics ascribed to I, II, and III in order to make actual calculations of their relative amounts. The overall results, however, are quite insensitive to the details.

For all conformers, we use the following notation. We refer to the 118 residues numbered 1–118 on each chain as region N of the molecule. In region N, each chain can form 118/3.5 = 33.7 helical blocks, which interact in the coiled coil with the strong, attractive free energy characteristic of the amino terminus, i.e., $-RT \ln w_N$ cal·(mol of block pairs)$^{-1}$. We refer to the 71 residues on each chain numbered 119–189 as region B. In region B, each chain can form 71/3.5 = 20.3 helical blocks. However, in region B, the interhelical interaction has been rendered repulsive; we write this interblock interaction free energy as $-RT \ln w_B$. Finally, we refer to the 95 residues on each chain numbered 190–284 as region C. In region C, each chain can form 95/3.5 = 27.1 helical blocks, which interact in a coiled coil with the weak, attractive free energy characteristic of the carboxyl terminus, i.e., $-RT \ln w_C$. Conformer I is the intact coiled coil. Conformer II differs from I only in that region B has unfolded to form a randomly coiled bubble. In conformer III, both regions B and N have unfolded.

In order to calculate the relative amounts of I, II, and III, we must assign numerical values to all parameters. The only parameter not yet so assigned is w_B. We therefore first write theoretical expressions for the standard chemical potential of each of the three species. Then, by considering the equilibrium I $\rightleftarrows$ II, we assign a numerical value to w_B such that, at 35 °C, II dominates, as required by the bubble hypothesis. Finally, we investigate the II $\rightleftarrows$ III equilibrium.

In the present theory, if the standard chemical potential of the completely random, cross-linked molecule is defined as zero, the value for I is given by (Skolnick, 1985b)

$$\mu_I^\theta/(RT) = -2 \ln \sigma - 2(284) \ln s - \ln r_\phi - 33.7 \ln w_N - 20.3 \ln w_B - 27.1 \ln w_C \quad \text{(A1)}$$

Each term on the right side of eq A1 has identifiable physical content. The first term is the free energy of initiating two independent helices; the second term is the free energy of propagating each independent helix for the full 284 residues; the third term is the free energy of initiating (lining up) the first pair of interacting helical blocks at the block containing the cross-link (Skolnick, 1985b); the fourth term is the free energy of propagating the interhelix interaction for the 33.7 helical blocks in the N region; the fifth (sixth) term is the free energy of propagating the interaction for the 20.3 (27.1) helical blocks in the B (C) region.

The standard chemical potential of conformer II is, in similar terms

$$\mu_{II}^\theta/(RT) = -2 \ln \sigma - 2(95) \ln s - \ln r_\phi - 27.1 \ln w_C - 2 \ln \sigma - 2(118) \ln s - \ln (C_1/142^{3/2}) - 33.7 \ln w_N \quad \text{(A2)}$$

In view of the discussion of eq A1, it is easily seen that the first four terms in eq A2 represent the contribution of the intact coiled coil at the C-terminus, i.e., residues 190–284; the next two give the contribution of the two individual helices at the N-terminus; the seventh term gives the contribution of initiating the first interacting block of the N-terminal coiled coil by formation of a 142-residue, randomly coiled loop and is expressed in terms of a statistically calculable parameter, C_1 (Skolnick, 1985b); the last term gives the free energy of propagating the interhelix interaction from residue 118 through residue 1 (N-terminus).

The foregoing allows us to write for the standard chemical potential of III, without further discussion

$$\mu_{III}^\theta/(RT) = -2 \ln \sigma - 2(95) \ln s - \ln r_\phi - 27.1 \ln w_C \quad \text{(A3)}$$

We next adjust w_B such that the equilibrium I $\rightleftarrows$ II is dominated by II at 35 °C. To this end, we use II/I = 10, giving

$$(\mu_{II}^\theta - \mu_I^\theta)/(RT) = -\ln (II/I) = -\ln 10 \quad \text{(A4)}$$

Obtaining the left-hand side of (A4) from (A1) and (A2) and rearranging, we obtain

$$20.3 \ln w_B = -\ln 10 + 2 \ln \sigma - 142 \ln s + \ln (C_1/142^{3/2})$$

At 35 °C, the appropriate numerical values are $\sigma = 5 \times 10^{-4}$, $s = 0.934$, and $C_1 = 0.2313$ (Skolnick, 1985b), giving

$$w_B = 0.439; \quad -RT \ln w_B \text{ (35 °C)} = 504 \text{ cal·(mol of block pairs)}^{-1} \quad \text{(A5)}$$

Thus, the local repulsion required is of about the same magnitude as the attraction is normally (Skolnick & Holtzer, 1985). If formation of the cross-link could lead to such a repulsion, the bubble structure II would indeed be considerably favored over the intact structure I at 35° C.

However, we next show that this would then inevitably lead to disabling other effects. The nature of these can be seen by considering the additional equilibrium II $\rightleftarrows$ III and calculating the equilibrium constant with (A2) and (A3). We find

$$(\mu_{III}^\theta - \mu_{II}^\theta)/(RT) = -\ln (III/II) = 2 \ln \sigma + 2(118) \ln s + 33.7 \ln w_N + \ln (C_1/142^{3/2}) \quad \text{(A6)}$$

Inserting the aforementioned values for σ, s (35 °C), and C_1, along with w_N(35 °C) = 3.22 (the latter obtained from eq 5), we obtain III/II = 2.24. Thus, the concentrations of our three prototypical species stand in the ratio of III:II:I of 22.4:10:1.

Consequently, if we provide a repulsion such that the amount of II dominates I, the theory requires that III be larger than II. The result, of course, is that the calculated helix content is far lower than the experimental value (75%) aimed for in the first place. If, using the same parameters, we make a more exact calculation, i.e., one in which all states are counted rather than only prototypical ones, the result is a helix content of only ~10%. This is totally at variance with the experiment.

We made many attempts at further adjustment without success. If the same repulsion is employed but one attempts to "correct" the low overall helix content by increasing w_C or w_N or both, then indeed one can reach 75% helix. Then, however, three other disastrous effects ensue: (1) Bubble-containing structures (like II) no longer dominate more intact ones (like I). In fact, bubbles simply disappear. (2) The numerical values required for w_N and w_C are then far larger than they are presently understood to be. (3) Use of the same (large) values for the non-cross-linked case, as would be demanded by self-consistency, then also raises *its* helix content so that the characteristic "double cross" of the experimental curves (Figure 1) is not mimicked by the theory.

There seems to be no way out. All our attempts to legislate bubbles resulted in failure. Such structures seem to be genuinely inconsistent with the present theory. Indeed, it would

require a drastic modification of the physics presently encompassed by the theory to produce such effects. Short of imagining that the cross-link somehow converts residues 119–189 into de facto prolines, we have no clue as to how to go about it.

REFERENCES

Betteridge, D., & Lehrer, S. (1983) *J. Mol. Biol. 167*, 481–496.

Chao, Y.-Y., & Holtzer, A. (1975) *Biochemistry 14*, 2164–2170.

Chen, C. L., & Skolnick, J. (1986) *Macromolecules 19*, 242–243.

Cohen, C., & Szent-Györgyi, A. G. (1957) *J. Am. Chem. Soc. 79*, 248–250.

Creighton, T. (1983) *Biopolymers 22*, 49–58.

Fraser, R., & Mac Rae, T. (1973) *Conformation in Fibrous Proteins*, Chapter 15, Academic, New York.

Graceffa, P., & Lehrer, S. (1980) *J. Biol. Chem. 255*, 11296–11300.

Graceffa, P., & Lehrer, S. (1984) *Biochemistry 23*, 2606–2612.

Halsey, J., & Harrington, W. (1973) *Biochemistry 12*, 693–701.

Harrington, W. F. (1979) *Proc. Natl. Acad. Sci. U.S.A. 76*, 5066–5070.

Holtzer, M. E., Holtzer, A., & Skolnick, J. (1983) *Macromolecules 16*, 173–180.

Holtzer, M. E., Breiner, T., & Holtzer, A. (1984) *Biopolymers 23*, 1811–1833.

Holtzer, M. E., Askins, K., & Holtzer, A. (1986) *Biochemistry 25*, 1688–1692.

Isom, L., Holtzer, M., & Holtzer, A. (1984) *Macromolecules 17*, 2445–2447.

Johnson, P., & Smillie, L. (1975) *Biochem. Biophys. Res. Commun. 64*, 1316–1322.

Lehrer, S. S. (1975) *Proc. Natl. Acad. Sci. U.S.A. 72*, 3377–3381.

Lehrer, S. S. (1978) *J. Mol. Biol. 118*, 209–226.

Lehrer, S. S. (1986) *Biophys. J. 49*, 258a.

Lehrer, S. S., & Betcher-Lange, S. (1979) *Motility in Cell Function*, pp 381–385, Academic, New York.

Lin, S., Konishi, Y., Denton, M., & Scheraga, H. (1984) *Biochemistry 23*, 5504–5512.

Mak, A., Lewis, W., & Smillie, L. (1979) *FEBS Lett. 105*, 232–234.

Mattice, W. (1980) *Macromolecules 13*, 506.

Noelken, M. (1962) Ph.D. Thesis, Washington University.

Noelken, M., & Holtzer, A. (1964) in *Biochemistry of Muscle Contraction* (Gergely, J., Ed.) pp 374–378, Little Brown, Boston.

Pato, M., Mak, A., & Smillie, L. (1981) *J. Biol. Chem. 256*, 593–601.

Pepe, F. (1967) *J. Mol. Biol. 27*, 203–225.

Poland, D., & Scheraga, H. (1970) *Theory of Helix-Coil Transitions in Biopolymers*, Chapter 9, Academic, New York.

Potekhin, S., & Privalov, P. (1982) *J. Mol. Biol. 159*, 519–535.

Scheraga, H. (1978) *Pure Appl. Chem. 50*, 315–324.

Skolnick, J. (1983a) *Macromolecules 16*, 1069–1083.

Skolnick, J. (1983b) *Macromolecules 16*, 1763–1770.

Skolnick, J. (1984) *Macromolecules 17*, 645–658.

Skolnick, J. (1985a) *Biochem. Biophys. Res. Commun. 129*, 848–853.

Skolnick, J. (1985b) *Macromolecules 18*, 1535–1549.

Skolnick, J. (1986) *Macromolecules 19*, 1153–1166.

Skolnick, J., & Holtzer, A. (1982a) *Macromolecules 15*, 303–314.

Skolnick, J., & Holtzer, A. (1982b) *Macromolecules 15*, 812–821.

Skolnick, J., & Holtzer, A. (1983) *Macromolecules 16*, 1548–1550.

Skolnick, J., & Holtzer, A. (1985) *Macromolecules, 18*, 1549–1559.

Stafford, W. (1985) *Biochemistry 24*, 3314–3321.

Stewart, M. (1975) *FEBS Lett. 53*, 5–7.

Ueno, H. (1984) *Biochemistry 23*, 4791–4798.

Williams, D., & Swenson, C. (1981) *Biochemistry 20*, 3856–3864.

Woods, E. F. (1969) *Int. J. Protein Res. 1*, 29–43.

Woods, E. F. (1977) *Aust. J. Biol. Sci. 30*, 527–542.

Yukioka, S., Noda, I., Nagasawa, M., Holtzer, M., & Holtzer, A. (1985) *Macromolecules 18*, 1083–1086.

Zimm, B., & Bragg, J. (1959) *J. Chem. Phys. 31*, 526–535.